Supporting Information

For the manuscript entitled:

Modeling Reaction Pathways for 2'OH Activation in RNA Catalysis: Metal-ion/Nucleobase Mechanisms in Self-Cleaving Ribozymes

Zdeněk Chval, [1,3*] *Daniela Chvalová,*[2] *Fabrice Leclerc*[3*]

[1] Department of Laboratory Methods and Information Systems, Faculty of Health and Social Studies, University of South Bohemia, J. Boreckého 27, 370 11 České Budějovice, Czech Republic

[2] Department of Applied Chemistry, Faculty of Agriculture, University of South Bohemia, Branišovská 31, 370 05, České Budějovice, Czech Republic

[3] Laboratoire ARN, RNP, structure-fonction-maturation, Enzymologie Moléculaire et Structurale (AREMS), UMR 7214 CNRS-UHP Nancy 1, Faculté des Sciences et Technologies, B.P. 70239, 54506 Vandoeuvre-lès-Nancy, France

S1. Mono-Anionic Mechanism

In the starting **IwH** structure the Mg^{2+} ion is coordinated to *pro-R_P* oxygen and five water ligands. The system is stabilized by two H-bonds of water ligands with *pro-S_P* and O2' oxygen atoms (Table S1 and Figure 3). In agreement with the study of Mayaan et al.[1] the coordination to the phosphate anion leads to an elongation of Mg-OH_2 coordination distances, which are longer than those in $[Mg(H_2O)_6]^{2+}$ by 0.015 Å in average (Mg-OH_2 = 2.124 Å). However, ligands which are involved in strong internal H-bonds show a reverse trend. In the case of **IwH,** two such H-bonds are formed between the coordinated water ligands and the *pro-S_P* and 2'O oxygen atoms, the corresponding Mg-OH_2 coordination distances are on the contrary shortened to 2.089 Å and 2.081 Å, respectively (Table S1). Coordinated *pro-R_P* oxygen also forms a nonlinear H-bond with the neighboring water decreasing the *pro-R_P*–Mg–OH_2 angle to 77.9 degrees. Disruption of the

symmetric octahedral arrangement of water ligands facilitates the change of the coordination number since smaller re-organization energy is required when switching between the penta- and hexa-coordinated forms. The penta-coordinated structure **IIIwH** with one water molecule in the second coordination shell is slightly more stable than the hexa-coordinated **IwH** structure by 2.5 kcal/mol on B3LYP/CPCM level. Note that MP2/CPCM shows the opposite trend (Table 2). The barrier for this process was determined to be 5.1 kcal/mol and 6.7 kcal/mol on DFT/CPCM and MP2/CPCM levels, respectively. The corresponding transition state **IIwH** has the Mg-OH_2 (leaving water) distance of 2.694 Å and the leaving water is already tilted to form two weak H-bonds with water ligands in the first coordination shell (Figure 3).

IIIwH has one water molecule in the second coordination shell. This water molecule is expected to have negligible influence on the next steps of reaction.[2] Therefore, it was omitted from our system and after a re-optimization **IIIH** was obtained. The relative energy level of **IIIH** was lined up to that of **IIIwH** to obtain a global estimate of the energy barrier of the coordination change step with respect to **IwH** (Figure 3). A penta-coordinated Mg^{2+} ion is then able to coordinate directly to the 2'-oxygen. The barrier for this process is 5.1 kcal/mol and the Mg-O2' distance is 2.725 Å in the **IVH** transition state (Figure 3 and Table 2). In **VH**, the 2'-oxygen is directly coordinated to the metal with the Mg-O2' distance of 2.161 Å. **VH** has almost the same energy than **IwH** (Figure 3 and Table 2) suggesting a fast equilibrium between the two states.

	Mg-O2P	Mg-2'O	Mg-H_2O					H-bonds	
			w1	w2	w3	w4	w5	w1-O2S	w2-2'O
IwH	2.004	3.924	2.089	2.081	2.132	2.158	2.162	1.600	1.677
IIwH	1.995	3.893	2.041	2.110	2.100	2.098	2.694	1.620	1.665
IIIwH	1.983	3.887	2.012	2.027	2.090	2.097	3.940	1.627	1.648
IIIH	1.976	3.850	2.028	2.022	2.080	2.128		1.564	1.640
IVH	1.963	2.725	2.063	2.071	2.145	2.082		1.594	1.993*
VH	1.992	2.161	2.091	2.102	2.144	2.129		1.602	2.173*

* nonlinear H-bond

Table S1: B3LYP/6-31+G* optimized main structural parameters of the Mg^{2+} coordination sphere of the structures along the Mono-Anionic pathway. Distances are given in angstroms, angles in degrees.

S2. Di-Anionic Mechanism

The OH^- hydroxyl anion in the first coordination shell of the Mg^{2+} ion was generated from **IwH** by removing a proton from a ligand water next to the 2'OH group. The resulting **Iw** structure (Figure 4) can be directly compared with the structure designated as '**I**' in the study about one-metal-ion mechanism of the HHR hydrolysis[3] (this structure is designated as **Iw2** in this study). According to our results, **Iw2** is not a global minimum and therefore the proposed one-metal-ion model is not energetically feasible due to too high activation free energy of ~30 kcal/mol (compare the relative energies of **Iw** and **TS-Ow** in Table 3). The deprotonation of the attacking 2'OH group and the protonation of the leaving group should be ensured by two independent species (in space and/or time): either a metal or a nucleobase, in agreement with the current experimental evidence.

IIIw has one water molecule in the second coordination shell with supposed negligible influence on the next steps of reaction.[2] Like in the case of Mono-Anionic mechanism the outer sphere water molecule was omitted from our system and after re-optimization we obtained the structure **III**. The relative energy level of **III** was lined up to that of **IIIw** to obtain a global estimate of the energy barrier of the coordination change step with respect to the starting **Iw** structure (Figure 4).

Going from **III** the subsequent coordination of 2'OH group to Mg^{2+} ion is followed by the proton transfer from 2'OH group (the Me-GB^{di} pathway). It was found that the final **VII** product structure can be reached by two possible pathways. Their starting structures differ only in the mutual position of the OH^- and *pro-*R_P ligands in the penta-coordinated magnesium complex. In **III**, both ligands occupy equatorial positions of the trigonal bipyramid. Due to large electrostatic repulsion between the two ligands the *pro-*R_P-Mg-$O(H)^-$ angle has not its ideal value of 120 degrees but is enlarged to 132.0 degrees. In the alternative **III-2** structure, the *pro-*R_P and OH^- groups are in the apical and equatorial positions, respectively. The O2P-Mg-$O(H)^-$ angle is even more distorted from the value of 90 degrees (from an ideal trigonal bipyramid) having value of 109.4 deg (Figure S2). The further mechanism of the reaction is rather similar in the two pathways, although the structures along the second pathway are slightly more stable (**III-2** is more stable than **III** by 1.4 kcal/mol: Table 3). The data corresponding to the second reaction pathway starting from **III-2** are given in parentheses in next two paragraphs and the course of reaction is shown in the Figure S2.

Bringing Mg^{2+} close to the O2' atom, the system needs to overcome a very small barrier of 0.22 kcal/mol (1.1 kcal/mol) to form hexa-coordinated **V** (**V-2**) structure with Mg-O2' distance of 2.336 Å (2.205 Å). The corresponding transition state **IV** (**IV-2**) has an imaginary frequency of –42.5 cm^{-1} (–76 cm^{-1}) and the Mg-O2' distance of 2.503 Å (2.585 Å) (Tables 3, S2 and Figures 4, S2).

After the coordination of O2' atom to Mg^{2+} ion in **V** (**V-2**), the subsequent H-transfer from the O2' atom to the OH^- group needs only a small barrier of about 0.17 kcal/mol (0.96 kcal/mol). In the transition state structure **VI** (**VI-2**) the transferred proton is shared by the $2'O^-$ and OH^- groups and the structure has an imaginary frequency of -779.3 cm^{-1} (–865.1 cm^{-1}). The $2'O^-$ nucleophile remains coordinated to the magnesium, the Mg-O2' distance is 2.208 Å (2.070 Å) (Figures S2 & 4). In the product structure **VII** the O2' atom is already firmly coordinated to Mg^2 with the distance of 2.013 Å. The P-O2' distance is decreased to 3.418 Å.

	Mg-O2P	Mg-2'O	Mg-OH^-	Mg-H_2O				H-bonds		
				w1	w2	w3	w4	w1-O2S	w2-2'O	2'OH-OH^-
Iw	2.044	3.370	2.014	2.153	2.159	2.166	2.171	1.712	1.798	1.615
Iw2	2.021	3.802	2.009	2.149	2.160	2.165	2.166			1.947
Iiw	2.047	3.264	1.977	2.199	2.158	2.126	2.464	1.760	1.800	1.641
IIIw	1.972	3.140	1.961	2.223	2.140	2.050	3.668	1.695	1.829	1.654
III	1.986	3.033	1.939	2.166	2.143	2.098		1.736	1.869	1.647
IV	2.029	2.503	1.945	2.136	2.155	2.125		1.698		1.639*
V	2.047	2.336	1.947	2.135	2.158	2.137		1.695		1.645
VI	2.034	2.208	2.033	2.116	2.156	2.136		1.694		
VII	2.025	2.013		2.132	2.169	2.147	2.149	1.652		
III-2	1.993	3.285	1.961	2.076	2.173	2.091		1.810	1.803	1.703
IV-2	1.997	2.585	1.980	2.102	2.212	2.108		1.671		1.696
V-2	2.036	2.205	2.009	2.111	2.175	2.157		1.680		
VI-2	2.030	2.070	2.126	2.101	2.154	2.156		1.660		

* nonlinear H-bond

Table S2: B3LYP/6-31+G* optimized main structural parameters of the Mg^{2+} coordination sphere of the structures along the Di-Anionic pathway. Distances are given in angstroms, angles in degrees.

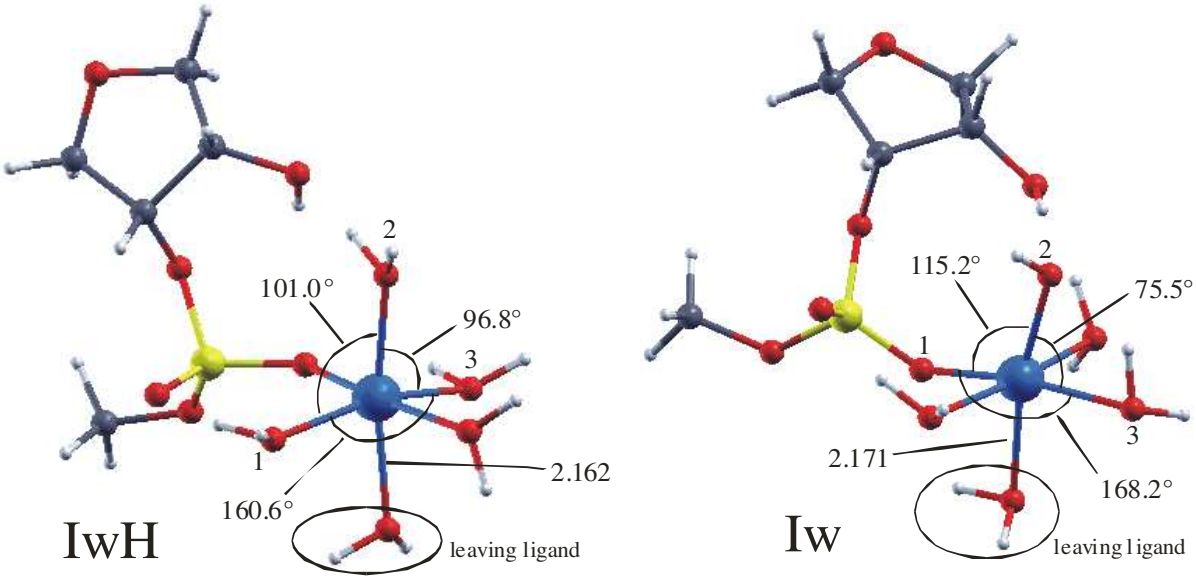

Figure S1: **Iw** and **IwH** structures: Mg-leaving_ligand bond is shorter in **IwH** structure than in **Iw** structure but the angles in the layout of the remaining ligands is closer to the trigonal bipyramidal geometry in the **IwH** structure than in the **Iw** structure expecting a need of smaller reorganization energy.

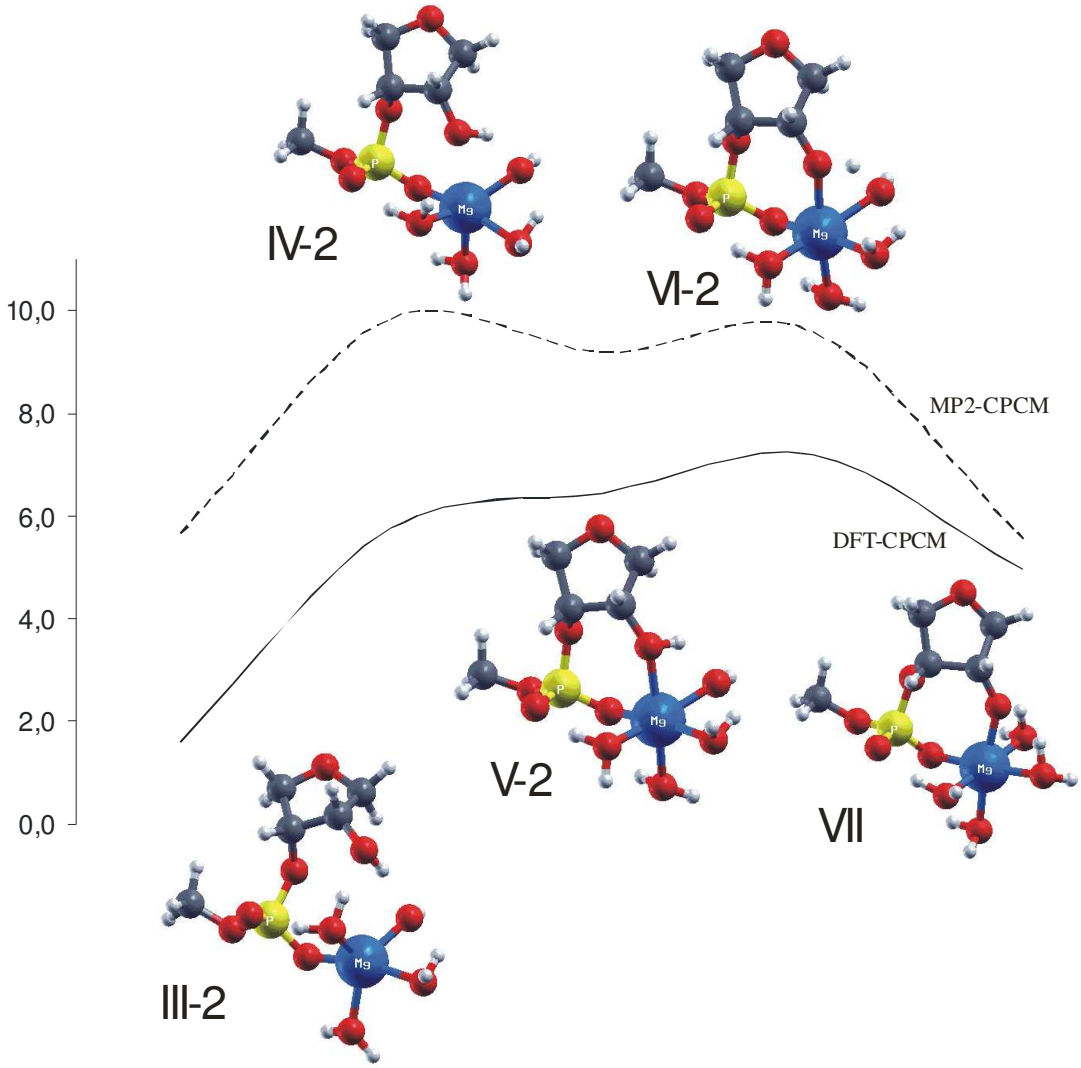

Figure S2: Potential energy surface for an alternative pathway for the Di-Anionic 2'O coordination and activation steps starting from **III-2** structure. Energies are relative to **Iw** structure (**IIIw** and **III** structures were set to be equivalent on the energy scale- see Table 2).

S3. Me-GB^{mono} Pathways with a subsequent cleavage reaction

The three M-GB pathways involve the 3'O, *pro-*R_P or *pro-*S_P oxygen atoms as possible internal bases for activation of the 2'OH in the **VH** structure. In the first pathway, the proton is transferred at first from 2'O to 3'O bridging oxygen followed by the transfer to 5'O of the leaving group. The rate-determining transition state (**TSH-O3** structure- see Figure 3) corresponds to the second transfer with a very high free energy difference of 54.5 kcal/mol with respect to the **VH** structure (Table 1).

In the intermediate structure **INT** the P-O5´ bond is already almost disrupted with a distance of 2.350 Å (P-2'O= 1.786 Å), but the leaving group is still associated to the 2'-3' cyclic phosphate. The reaction then proceeds via the final transition state **TS-2** (P-O5´ = 2.697 Å; P-2'O= 1.723 Å) to the **PROD** product structure where the leaving group enters into the second coordination shell of the Mg^{2+} ion. The 2'O oxygen leaves the first coordination shell of the Mg^{2+} ion when the P-2'O bond is formed (Figure 3) as it was also observed in other models.[3,4] Note that the potential energy surface is rather flat in the region of the **INT** and **TS-2** structures. According to B3LYP/6-31+G* energies the **INT** structure is by 0.6 kcal/mol more stable than **TS-2**. When larger basis sets are used, the **TS-2** structure is in fact more stable than the **INT** structure (Table 1). Despite an uncertainty in geometries of **INT** and **TS-2** structures, our results clearly show that CH_3O-H is a good leaving group (as expected) and the cleavage proceeds smoothly when the methoxy CH_3O^- group is protonated.

The alternative pathways where the internal base is one of the non-bridging oxygens (*pro-R_P* or *pro-S_P*) are more favorable with activation free energies of 43.7 and 42.4 kcal/mol (transition states **TSH-OR** and **TSH-OS**, respectively- Figure 3 and Table 1). These values are in excellent agreement with the value of 44.7 ± 2.3 kcal/mol that was calculated by Boero et al.[5] by the Car-Parrinello MD simulation for a proton transfer from 2'O to 5'O oxygen via *pro-S_P*. Since 2'OH group has only water-mediated contacts with *pro-R_P* and *pro-S_P* atoms, a determination of full reaction pathways would be rather complicated due to the existence of several intermediates and these were not localized. Only transition states **TSH-OR** and **TSH-OS** for a final proton transfer to 5'O from *pro-R_P* and *pro-S_P* oxygen atoms, respectively, were optimized (Figure 3) since the formation of the leaving group is the rate-determining step for the cleavage reaction.[3-6]

S4. A comparison of the Me^i-GB^{di} mechanism with the Torres´ one-metal-ion model[3] (Me^o-GB^{di} mechanism)

Iw2 and **Iw** structures differ in the H-bond interaction pattern between $Mg^{2+}(H_2O)_4(OH^-)$ and ribozyme subunits (Figure S3). In both structures Mg^{2+} ion is directly coordinated to *pro-R_P* oxygen atom. 2'OH and (OH^-) groups are in a good mutual position with respect to the future H-transfer between these groups. However, **Iw** structure offers much more advantageous H-bond interactions than **Iw2** structure. In the former structure, more energetically favorable contacts of metal ligands with 2'O and non-bridging *pro-S_P* oxygen atoms are established while in the latter structure the metal ligands form contacts with bridging 5'O and 3'O oxygen atoms. Moreover, the same other three H-bonds are formed in both structures and all these H-bonds are also shorter in **Iw** structure

(Tables S2 and S3). The **Iw** structure is by 11.8 kcal/mol and by 9.3 kcal/mol more stable than structure **Iw2** using B3LYP/CPCM and MP2/CPCM method, respectively (Table 2). Structure **Iw2** was derived on the base of standard molecular dynamics calculations[7,8] which do not include non-electrostatic polarization and charge transfer interactions. Classical force field calculations may fail to predict an optimal hydrogen bonding pattern between hydrated Mg^{2+} ion and a nucleic acid structure.[9] The polarized water molecules belonging to the cation hydration shell are capable of forming H-bonds that are considerably stronger than those usually formed by water. The stronger nucleophile is involved in H-bonding the more important is the difference between polarized and nonpolarized water molecules.[10]

These assumptions can be supported by the fragment energy decomposition analysis (see bellow for details). It reveals that differential energy of 23.8 kcal/mol separating **Iw** and **Iw2** structures can be attributed to the more advantageous orbital interaction (i.e. polarization and charge transfer) contributions between the two fragments in **Iw** structure while the difference in electrostatic interaction is almost fully diminished by Pauli repulsion (Table S4).

	Iw			Iw2		
	length (Å)	O-H bond distances in H-bond donor group[c]		length (Å)	O-H bond distances in H-bond donor group[c]	
HO···HO‘2	1.615	1.013	-	1.947	0.986	-
O_S···HOH[a] vs. O5‘···HOH[b]	1.712	1.007	0.969	1.865	0.987	0.970
HO···HOH	1.783	1.000	0.970	1.840	0.996	0.970
O‘2···HOH[a] vs. O‘3···HOH[b]	1.798	0.992	0.971	1.929	0.982	0.981
O_R···HOH	2.025	0.981	0.970	2.049	0.979	0.969

Table S3: Comparison of hydrogen bonds in the Iw and Iw2 structures, respectively.

[a] a hydrogen bond in the Iw structure

[b] a hydrogen bond in the Iw2 structure

[c] Distance comparison of lengths of O-H bonds in H-bond donor group (it is water with exception of the first row where it is OH^- ligand). In the first column is the O-H bond what takes part in the H-bond is shown. Its relative prolongation with respect to the other bond is in proportion to the strength of the H-bond.

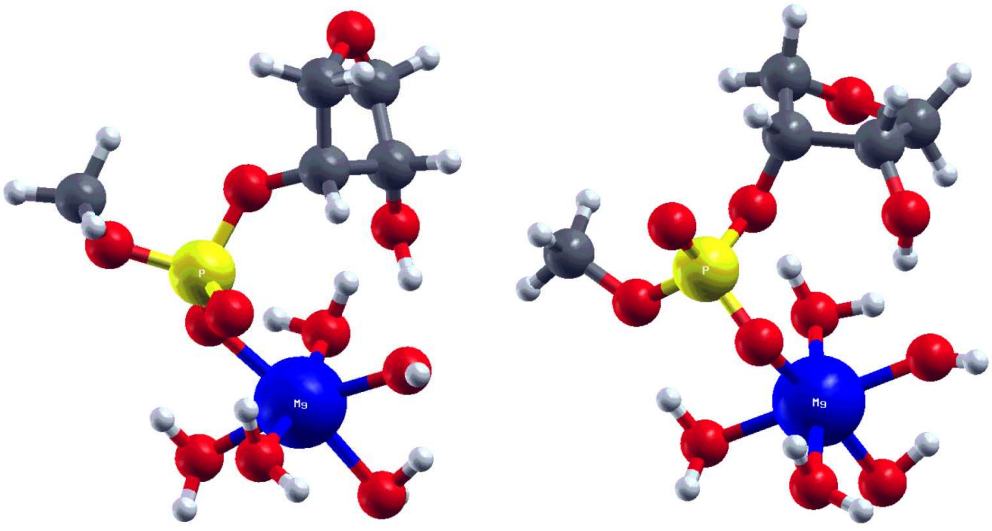

Iw structure **Iw2 structure**

Figure S3: A comparison of the **Iw** and **Iw2** structures.

S5. Energy decomposition analysis of selected structures

The fragment calculations available in ADF provide a decomposition of the binding energies in a chemically meaningful manner.[11] Table 5 shows energy terms according to the Ziegler-Rauk decomposition scheme of the selected structures. The 'RIB' fragment presents the ribose phosphate and 'MG' fragment contains Mg^{2+} ion with its water H_2O and hydroxo OH^- ligands. Note that total interaction energy corresponds to the bond energy of the fragments with geometries as found in the original molecule. Thus the fragments are not at their equilibrium geometry resulting in much higher bond energies comparing to that of true overall bond energy (the energy difference is usually called the preparation energy and is the energy needed to deform the equilibrium geometries of the separate fragments to that found in the adduct structure). The interaction energy can be further decomposed into three terms:

$$\Delta E_{\text{int}} = \Delta E_{Pauli} + \Delta E_{el-st.} + \Delta E_{orb-\text{int}}$$

The term ΔE_{Pauli} comprises the destabilizing interactions between occupied orbitals in accord with the Pauli principle. The second term $\Delta E_{el-st.}$ corresponds to the classical electrostatic interaction between the charge distributions of the two fragments. Finally, the orbital interaction $\Delta E_{orb-\text{int}}$ accounts for charge-transfer and polarization interactions.

The $\Delta E_{el-st.}$ term represents the main part of the interaction energy, and it is strongly dependent on the charge of the fragments. Orbital interaction term $\Delta E_{orb-\text{int}}$ is very important too and it involves about 45% of the total interaction energy for the structures with fragment charges q(RYB) = -1e and q(MG) = +1e. For the structures with fragment charges: q(RYB) = -1e; q(MG) = +2e and q(RYB) = -2e; q(MG) = +2e the importance of $\Delta E_{orb-\text{int}}$ term for decreases down to 35% and 30%, respectively. Relatively high relevance of the latter is caused by its strong increase in structure **VII** due to direct coordination of activated O2´ to Mg^{2+} and high mutual polarization of the fragments. Note that this analysis is done in the gas phase. In a real solution, a relative relevance of the non-electrostatic term is further increased since it is almost unaffected by a change of the environment. On the other hand, the electrostatic component is reduced substantially (we have shown that the influence of electrostatic charges on total interaction energy can be completely diminished in the water environment[12]). This trend can be seen already by a comparison of **IIIwH** and **IIIw** structures with **IIIH** and **III** structures, respectively. A second coordination shell water deletion when going from the former to the latter structures leads to higher total interaction energy mainly due to higher

electrostatic interaction caused by fewer effective screening of Mg^{2+} charge. In case of Mg^{2+} coordination to 2'OH group the orbital interaction is lowered by about 10 kcal/mol.

Structure	Q(RYB)[a]	Q(MG)[a]	E(Pauli)	E(el-stat)	E(nonorb-int)	E(orb-int)	E(tot)
IwH	-1	2	64.0	-261.3	-197.4	-110.2	-307.5
IIIwH	-1	2	63.6	-259.1	-195.5	-110.2	-305.7
IIIH	-1	2	62.8	-266.5	-203.7	-111.9	-315.6
IVH	-1	2	59.7	-270.7	-211.0	-110.7	-321.7
VH	-1	2	64.6	-276.9	-212.3	-118.0	-330.3
Iw	-1	1	85.6	-206.6	-121.0	-106.7	-227.8
Iw-2	-1	1	58.3	-176.0	-117.6	-86.3	-204.0
IIIw	-1	1	81.1	-204.5	-123.4	-104.5	-227.9
III	-1	1	82.2	-209.4	-127.2	-102.9	-230.1
IV	-1	1	85.7	-216.2	-130.5	-107.2	-237.8
V	-1	1	86.5	-217.6	-131.1	-109.2	-240.2
VII	-2	2	105.3	-512.2	-406.9	-172.1	-579.0
III-2	-1	1	77.6	-199.9	-122.3	-97.5	-219.9
IV-2	-1	1	79.0	-204.2	-125.2	-101.8	-227.1
V-2	-1	1	85.8	-209.8	-124.0	-108.3	-232.3

Table S4. Ziegler- Rauk energy decomposition of the MG-RIB interaction (see the text) for selected structures (all energies are given in kcal/mol).

[a] Net charges of RIB and MG fragments.

S6. Me-SB Pathway

A hydroxide OH^- ion was added to the second coordination shell of Mg^{2+} ion in **VH** (see above) to obtain the **VHOH** structure (Table 3 and Figure 5). In **VHOH**, two proton transfers are possible to the external OH^- group: from the 2'OH (2'OH activation) or from an equatorial metal-coordinated water ligand (forming metal coordinated hydroxide, which may activate 2'OH in the next step following the **Me-GB^{di}** pathway as described previously).

The stationary points along the pathway have very close energy levels but the equilibrium should be slightly shifted towards to the 2'OH deprotonation. This is in agreement with results from

previous paragraphs.[13] Both proton transfers: from 2'OH to OH^- and from H_2O to OH^- are almost barrierless. In the gas phase, both transition states **VIw** and **Vw2** are slightly more stable than the reactant structure **VHOH** after inclusion of ZPE and thermal corrections. The **Vw2** transition state structure[4] for $(Mg)OH_2 \rightarrow OH^-$ proton transfer is even more stable than **Vw3** being the lowest structure on this part of the potential energy surface (Table 3 and Figure 5), indicating that the proton is most likely shared by the two groups. Solvation corrections disadvantage the transition states structures more than **VHOH**. The maximum energy difference between the structures for the $(Mg)OH_2 \rightarrow OH^-$ proton transfer pathway is 0.6 kcal/mol. The 2'OH → OH^- proton transfer is more clearly spontaneous since **VIIw** is more stable than **VHOH** by up to 1.97 kcal/mol (for MP2/CPCM).

The pKa value of the 2'OH group directly coordinated to Mg^{2+} ion can be estimated by a comparison of relative energies of the **VIIw** and **Vw3** structures (Figure 5). **VIIw** structure is always more stable and the energy difference ranges from 0.68 kcal/mol (DFT/CPCM) up to 2.30 kcal/mol (MP2/CPCM) (Table 3). Therefore, the pK_a value of the 2'OH group should be by 0.5 - 1.7 units lower (the lower and higher values correspond to DFT/CPCM and MP2/CPCM difference, respectively) than the pK_a value of a magnesium water ligand. This result seems to be realistic since the difference between pK_a values of Mg^{2+} coordinated 2'OH and water ligands is roughly the same as the difference between pK_a values of a free 2'OH group and water molecule (14.9 (ref. 15) – 15.7 = -0.8). Recent kinetic experiments on the *S. mansoni* hammerhead ribozymes[6] show 344 times (0.86 vs. 0.0025) lower value of the first-order rate constant for the 2'-deoxy-G8 mutant comparing to the wild type ribozyme in the presence of the Mg^{2+} cofactor. It corresponds to the activation energy difference of 3.6 kcal/mol and it is explained[16] by the pK_a value difference between Mg^{2+} coordinated 2'OH and water ligands.

The rationale from the previous paragraph supposed one deprotonation event on one specific site. For systems with multiple deprotonation sites, it is reasonable assumption only when they form a strong H-bond with a general base and deprotonation occurs along this H-bond. However, if one wants to estimate the pK_a value of 2'OH on the base of the known pK_a value of Mg^{2+} bound water (11.4[17]) we have to take into consideration that this value was measured for $[Mg(H_2O)_6]^{2+}$ complexes that have twelve equivalent deprotonation sites. If we suppose that acidity of the Mg^{2+} bound water ligands is the same in the **Vw3** and $[Mg(H_2O)_6]^{2+}$ complexes (what however might not be exactly true) then the mean pK_a value of one specific deprotonation site can be estimated by adding a correction factor of log(12*2) = 1.4 to the value of 11.4. Therefore, if the above assumptions are valid the pK_a value of the coordinated 2'OH group should be in the range 11.1 –

12.3. Thus again the Mg^{2+} coordination to 2'OH lowers the pK_a value of the 2'OH group by about three log units.

Iw is an isomer of **VHOH** and their relative energy should give information about the stability of inner and outer shell coordination of 2'OH and OH^- ligands to the Mg^{2+} ion (Table 3). Although the OH^- group is well stabilized by three strong H-bonds with 2'OH (1.553 Å) and two polarized water ligands (1.539 Å; 1.589 Å) in **VHOH**, the inner shell coordination of the OH^- group in **Iw** is preferred by more than 4 kcal/mol due to more favorable electrostatics.

S7. Nucleobase-dependent activation

Nu-GB^{di} Pathway. The starting **RG-R** structure is derived from the X-ray structure of a full-length catalytically active hammerhead ribozyme (2GOZ structure[18] in the Protein Data Bank). **RG-R** consists of the phospho-ribose moiety of C-17 and the N1-deprotonized guanine base (G_{DP}) with a bound water molecule to O6 (the O6-OH_2 distance is 2.42 Å (Figure S4). The presence of this water molecule facilitates probably a deprotonation of the imino N1-H group since the engagement of O6 in strong H-bonding makes the imino proton more acidic.[19]

In **RG-R,** the N1 atom of G_{DP} is within a hydrogen bonding distance of the 2'OH nucleophile of C-17.[18] With respect to the initial X-ray structure the N1-2'O distance was shortened from 3.53 Å to 2.82 Å and the phosphate terminus was rearranged after optimization due to the H-bond formed between the O3' oxygen and the exocyclic amino group (the O3'-N2 distance was shortened from 6.34 Å to 3.15 Å). The in-line conformation found in the crystal structure was not preserved (Figure S4).

The proton transfer occurs early along the reaction: in the transition state structure **RG-TS,** the proton is almost bound to N1 (N1-H and O2'-H distances are 1.156 Å and 1.405 Å, respectively) suggesting a strongly endothermic profile according to Hammond's postulate (Figure 6). Increased negative charge on the O2' atom is stabilized by the formation of a strong H-bond with the exocyclic amino group of guanine (O2'···NH2 distance is 1.860 Å). The activation energy for the O2'→N1 proton transfer is 6.6 kcal/mol (Table 4).

In the product **RG-P**, the activated nucleophile is stabilized by two strong H-bonds O2'···H(NH2) (1.605Å) and O2'···H(N1) (1.785Å), (Figure S4). The proton transfer is endothermic with an energy variation of 7.09 kcal/mol. The product is not more stabilized than the transition state (**RG-P** vs **RG-TS**: Table 4). The product can be further stabilized by positively charged species (e.g. a directly coordinated metal ion) not considered in this reaction mechanism, assuming the reaction is

sequential. Otherwise, the poor stabilization of RG-P can be advantageous in case the 2'OH activation is concerted with the protonation of the O5' atom from the leaving group.

Nu-GB^{mono} Pathway. The in-line conformation is well reproduced in **RGwR** when the negatively charged phospho-ribose moiety is bound to the neutral enol-tautomer of G12 (G_{NE}) and a structural water molecule is added in-between the polar and charged groups: the exocyclic amino group of G_{NE} and the phosphate group (Figure S4). The relative orientation of G_{NE} and the phospho-ribose moiety deviated from the X-ray structure reinforcing the interaction between the O6-H enol group and the pro-R_p oxygen (O6- pro-R_p = 2.57 Å). The N1-O2' distance is shortened to 2.91 Å. The structural water molecule stabilizes the complex by H-bonds with pro-S_p and O2' oxygen atoms and with the exocyclic amino group.

The product structure (**RGwP**) is obtained through two concerted proton transfers: from 2'OH to the imino nitrogen N1 of G-12 and from the exocyclic O6 of G_{NE} to the non-bridging pro-S_p oxygen (O2'$\cdots$H-N1 = 1.467 Å; H-N1 = 1.108 Å; O6$\cdots$H- pro-S_p = 1.661 Å; H- pro-S_p = 1.009 Å) (Figure S4). The O6 → pro-S_p proton transfer is also observed using an implicit solvent model in complementary calculations at the CPCM/B3LYP/6-31+G* level, suggesting it is not an artifact of the gas phase optimization. As a result, G_{NE} is converted into its standard tautomeric form and the overall change on the ribose is equivalent to a direct O2' → non- bridging oxygen proton transfer. The reaction is strongly endothermic: ΔG_r^0 = 12.86 kcal/mol (Figure 6).

The transition state **RGwTS** structure has almost the same geometry as **RGwP** (O2'$\cdots$H-N1 = 1.371 Å; H-N1 = 1.154; O6$\cdots$H- pro-S_p = 1.627 Å; H- pro-S_p = 1.014). The activation energy is 12.58 kcal/mol (Figure 6). In fact, **RGwTS** is slightly more stable than **RGwP** (0.3 kcal/mol) at the B3LYP/6-311+G(2d,2p)//6-31+G* level suggesting a stretching of the H-N1 bond when optimizing RGwP structure with a more flexible basis set than 6-31+G*. Therefore, a similar trend is also observed where the equilibrium of the reaction is displaced towards the reactant (reverse reaction) rather than towards the product (forward reaction).

Nu+Me-GB^{di} pathway. In the last activation mode, we have studied the influence of a hydrated metal ion on the energetics of the proton transfer. Due to the complexity of the system, all the structures along the Nu+Me-GB^{di} pathway were optimized at the HF/3-21+G* level but single point calculation were performed at the B3LYP/6-311+G(2d,2p) level both in the gas phase and in solution using an implicit solvent model.

In the starting **RGM-R** structure the Mg^{2+} ion is directly coordinated to pro-R_P oxygen (Figure S4). The 2'OH group is solvated by two explicit water molecules: the first one is from the inner-

sphere coordination shell and the second one is from the outer-sphere coordination shell of the Mg^{2+} ion (the H-O2'···H distances are 1.882 Å and 1.806 Å, respectively). Another water molecule was added to stabilize the negative charge on the O6 atom of G_{DP} (O6···H = 1.601 Å).

In the transition state **RGM-TS** the proton is almost symmetrically shared by the O2' and N1 atoms (O2'-H = 1.197Å; N1-H = 1.291Å), (Figure 6). Actually, the proton sharing may occur spontaneously at the CPCM/B3LYP/6-311+G(2d,2p)//HF/3-21+G* level since **RGM-TS** is the lowest energy structure (Table 4). In the product structure (**RGM-P**), the proton is fully transferred to N1 (N1-H = 1.043Å; O2'···H = 1.632Å). The proton transfer is slightly endothermic by 2.58 kcal/mol.

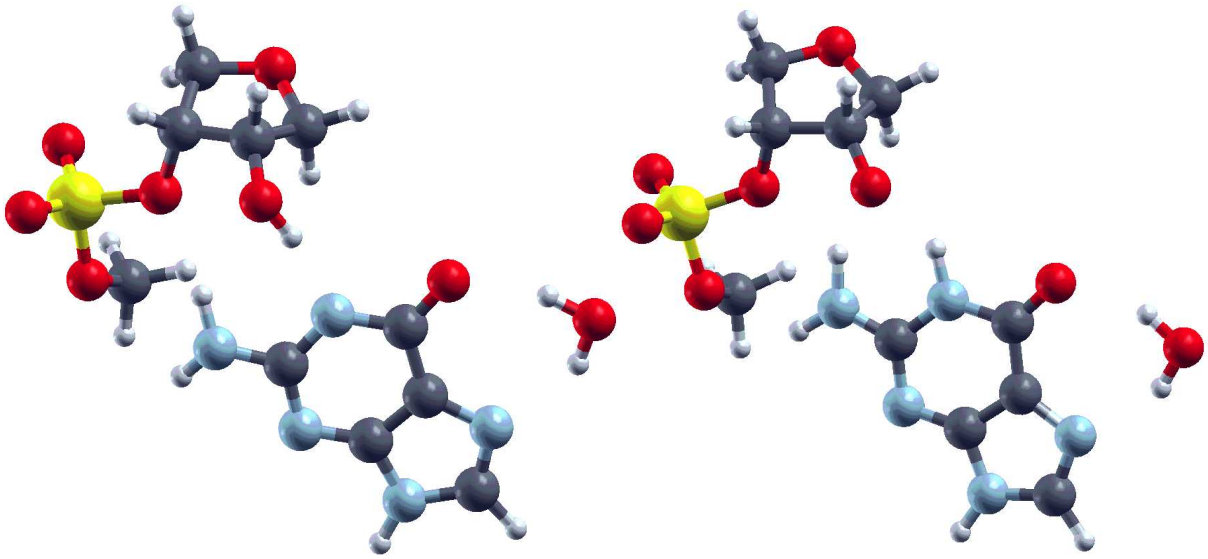

RG-R **RG-P**

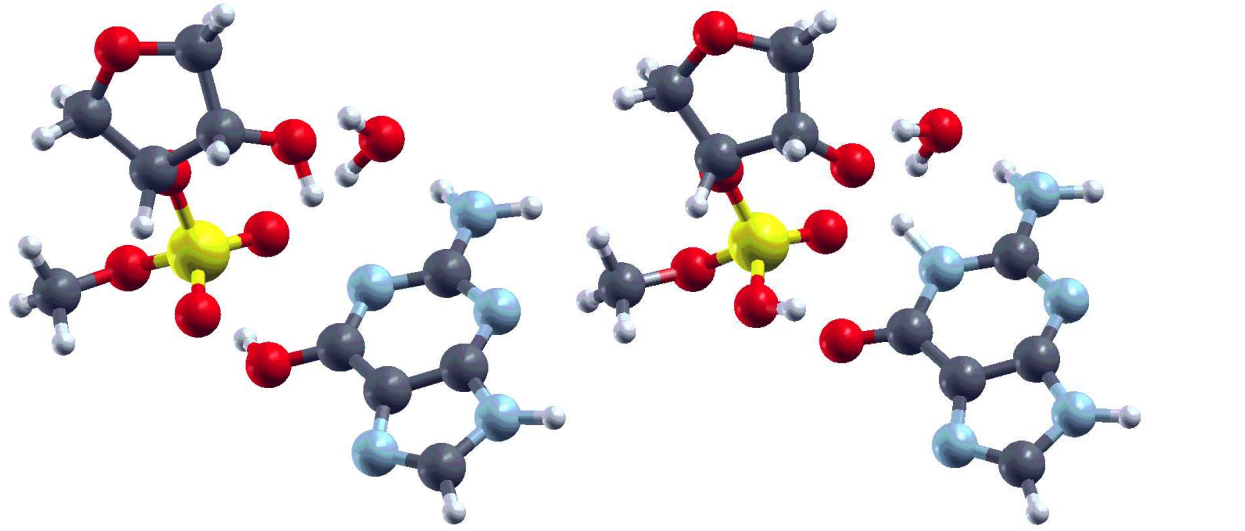

RGwR **RGwP**

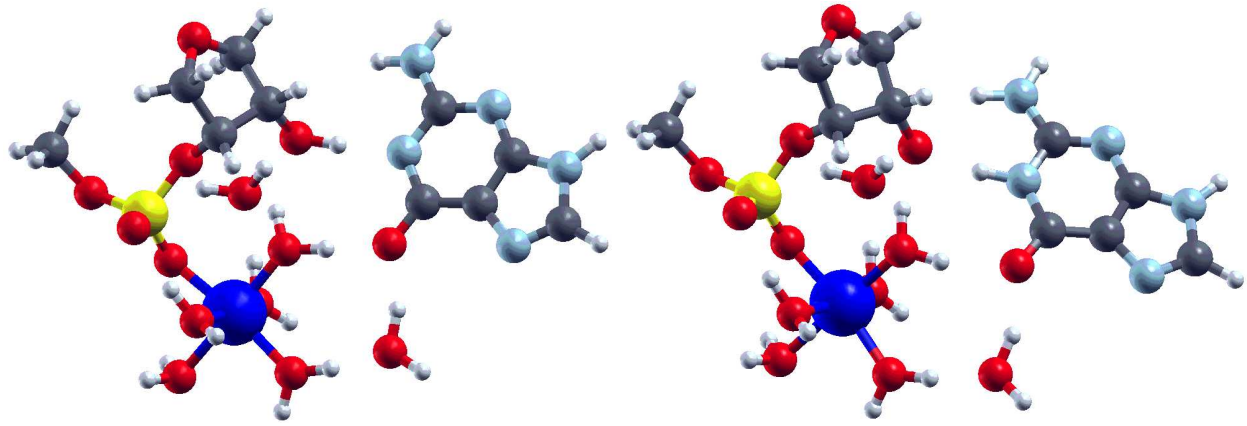

RGMR **RGMP**

Figure S4: Structures related to the N-SP and N-SP+M pathways

References and Notes:

(1) Mayaan, E. Range, K.; York, D. *J. Biol. Inorg. Chem.* **2004**, *9*, 807-817.

(2) Deletion of the water molecule from the 2nd coordination shell may lead to closer contacts between hydrated Mg^{2+} and a ribozyme unit in the gas-phase optimized structures due to slightly less effective screening of the magnesium charge (compare structural parameters of **IIIwH** structure with **IIIH** structure in Table 1). However mutual orientation of ligands in the first coordination shell is unaffected. When deleting the water molecule from the 2nd coordination shell from the **IIIwH** and **IIIw** structures to obtain **IIIH** and **III** structures the energy gain due to optimization was 2.10 and 2.76 kcal/mol,

(3) Torres, R.; Himo, F.; Bruice, T.; Noodleman, L.; Lovell, T. *J. Am. Chem. Soc.* **2003**, *125*, 9861-9867.

(4) Leclerc, F.; Karplus, M. *J. Phys. Chem. B* **2006**, *110*, 3395-3409.

(5) Boero, M.; Tateno, M.; Terakura, K.; Oshiyama, A. *J. Chem. Theory Comput.* **2005**, *1*, 925-934.

(6) Takagi, Y.; Warashina, M.; Stec, W.; Yoshinari, K.; Taira, K. *Nucleic Acids Res.* **2001**, *29*, 1815-1834.

(7) Torres, R.; Bruice, T. *Proc. Natl. Ac. Sc. USA* **1998**, *95*, 11077-11082.

(8) Torres, R.; Bruice, T. *J. Am. Chem. Soc.* **2000**, *122*, 781-791.

(9) Petrov, A. S.; Pack, G. R.; Lamm, G. *J. Phys. Chem. B* **2004**, *108*, 6072-6081.

(10) Sponer, J.; Sabat, M.; Gorb, L.; Leszczynski, J.; Lippert, B.; Hobza, P. *J. Phys. Chem. B* **2000**, *104*, 7535-7544.

(11) Velde, G. T.; Bickelhaupt, F. M.; Baerends, E. J.; Guerra, C. F.; Van Gisbergen, S. J. A.; Snijders, J. G.; Ziegler, T. *J. Comput. Chem.* **2001**, *22*, 931-967.

(12) Chval, Z.; Sip, M.; Burda, J. *J. Comput. Chem.* **2008**, *29*, 2370-2381.

(13) Comparing relative energies of **VIIw** and **Vw3** structures with relative energies of **VII** and **V** structures, respectively, one gets similar results. The former structures differ from the latter ones only by one water molecule in the second shell.

(14) Roman numerals in **Vw2** and **Vw3** designations refer to the stage of the reaction with respect to the 2'OH activation mechanism. 2'O is already coordinated to the Mg^{2+} ion but it is not activated by a hydrogen transfer, i.e. the reaction is in the same stage as **V** and **V-2** structures.

(15) Lyne, P.; Karplus, M. *J. Am. Chem. Soc.* **2000**, *122*, 166-167.

(16) Thomas, J.; Perrin, D. *J. Am. Chem. Soc.* **2009**, *131*, 1135-1143.

(17) Pan, T; Long, D.M.; Uhlenbeck, O.C. *Divalent Metal Ions in RNA folding and Catalysis*; Cold Spring Harbor Press: Plainview, NY, 1993.

(18) Martick, M.; Scott, W. *Cell* **2006**, 126, 309-320.

(19) Lippert, B. *Chemistry & Biodiversity* **2008**, 5, 1455-1474.